Magnetic Properties of Polystyrene-*b*-Poly(2-hydroxylethyl methacrylate)/Metal Hybrids

Yanmei Wang, Ruping Zhu, Weidong He

Department of Polymer Science and Engineering, University of Science and Technology of China, Hefei, 230026, People's Republic of China

Received 14 July 2004; accepted 13 April 2005
DOI 10.1002/app.22731
Published online 14 December 2005 in Wiley InterScience (www.interscience.wiley.com).

ABSTRACT: Hybrids, which were composed of the amphiphilic diblock copolymer polystyrene-*b*-poly(2-hydroxylethyl methacrylate) (PSt-*b*-PHEMA) and nickel, cobalt, or a nickel–cobalt alloy, were characterized with infrared absorption spectroscopy and ultraviolet–visible (UV–vis) absorption spectroscopy. UV–vis spectroscopy analysis showed that a redshift happened after the PSt-*b*-PHEMA/metal-ion complexes were reduced by KBH_4. The PSt-*b*-PHEMA/nickel–cobalt alloy hybrids had the biggest redshift [difference of the UV-vis absorption wavelength between (PSt-*b*-PHEMA)/metal ion complex and (PSt-*b*-PHEMA)/metal hybrids ($\Delta\lambda_m$ = 19.9 nm)]. In comparison with the PSt-*b*-PHEMA/nickel hybrids ($\Delta\lambda_m$ = 3.5 nm) and PSt-*b*-PHEMA/cobalt hybrids ($\Delta\lambda_m$ = 9.0 nm). The magnetic properties of PSt-*b*-PHEMA/metal were studied with vibrating sample magnetometry. The results of magnetic hysteresis loop studies showed that the obtained PSt-*b*-PHEMA/metal hybrids could be categorized as ferromagnetic materials. The results showed that the magnetic susceptibility decreased with increasing temperature in the range of 150–400 K and increased with increasing temperature above 400 K. © 2005 Wiley Periodicals, Inc. J Appl Polym Sci 99: 2314–2319, 2006

Key words: amphiphiles; diblock copolymers; magnetic polymers

INTRODUCTION

Because there are strong chemical bonds (covalent or ionic) or interactions such as van der Waals forces, hydrogen bonding, and electrostatic forces in polymer/metal hybrids,[1] some properties of polymer/metal hybrids, such as optical, magnetic, catalysis, and electronic properties, are different from those of the pure polymers and pure metals.[2,3] To control the functionality of these composite materials, the location and size of metal nanoclusters in the gels should be controlled. Microphase separation of amphiphilic block copolymer results in heterogeneous structures with, for example, lamellae, cylinders, or spherical microdomains, which can serve as nanoreactors within which a variety of nanoclusters can be synthesized in a controlled manner.[4–7] The geometry and size of the nanoreactor usually can be varied in a predictable manner by the adjustment of the length of each block and the total molecular weight.[8] Thus, the properties of amphiphilic block copolymer/metal hybrids can be controlled through the control of the structure of the block polymer. Advantageous use of such structures has been made for the production of a variety of nonmagnetic metal nanoclusters (Ag, Au, Pd, and Pt)[8–12] and magnetic nanoclusters.[13,14]

Recently, we reported a method for synthesizing polystyrene-*b*-poly(2-hydroxylethyl methacrylate) (PSt-*b*-PHEMA) nickel, cobalt, and nickel–cobalt alloy hybrids.[15] First, the block copolymer polystyrene-*b*-poly-[2-(trimethylsilyoxy)ethylene methacrylate] (PSt-*b*-PTMSEMA) was synthesized with atom transfer radical polymerization (ATRP). ATRP has been proven to be effective for a wide range of monomers[16,17] and appears to be powerful for controlling the polymer molecular weight and distribution. Then, the hydrolysis of PSt-*b*-PTMSEMA led to the formation of an amphiphilic diblock copolymer, PSt-*b*-PHEMA. Transmission electron microscopy (TEM) showed that the obtained PSt-*b*-PHEMA ($[St]_{117}[HEMA]_{21}$) formed micellar aggregates, with the insoluble block polystyrene (PSt) as the core and the soluble block poly(2-hydroxylethyl methacrylate) (PHEMA) as the corona, in the mixed solvents dimethylformamide (DMF) and water. Under appropriate conditions, the addition of Co^{2+} and Ni^{2+} ions to the PSt-*b*-PHEMA solution in DMF and water greatly affected the microphase-separation process and, lastly, the morphologies of the metal-ion/polymer composite. Electron spectroscopy for chemical analysis (ESCA) and X-ray diffraction (XRD) analysis showed that before reduction the metal existed as

Correspondence to: Y. Wang (wangyanm@ustc.edu.cn).
Contract grant sponsor: National Natural Science Foundation of China; contract grant number: 59903006.
Contract grant sponsor: Natural Science Foundation of Anhui Province; contract grant number: 01044906.

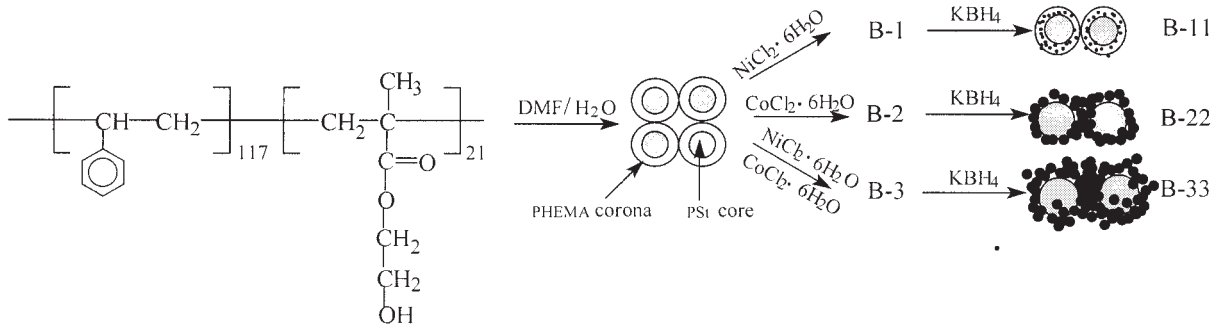

Scheme 1 Preparation process of the PSt-*b*-PHEMA/nickel-ion complex (B-1), PSt-*b*-PHEMA/cobalt-ion complex (B-2), PSt-*b*-PHEMA/nickel–cobalt-ion complex (B-3), PSt-*b*-PHEMA/nickel hybrids (B-11), PSt-*b*-PHEMA/cobalt hybrids (B-22), and PSt-*b*-PHEMA/nickel–cobalt hybrids (B-33).

a hydroxide; after reduction with KBH_4, nanometer metal particles [Ni(0) or Co(0)] on the surface were formed and oxidized in air to form NiO or CoO. TEM showed that most of these metals were aggregated.

This article presents research continuing from our previous work.[15] The goal of this research is studying the magnetic properties of $[St]_{117}[HEMA]_{21}$ metal (cobalt, nickel, and cobalt–nickel alloy) hybrids. The magnetic behavior of the hybrids was examined with vibrating sample magnetometry (VSM) at temperatures ranging from 78 to 423 K and at fields ranging from 0 to 5 kOe.

EXPERIMENTAL

Materials

PSt-*b*-PHEMA/metal hybrids containing nickel, cobalt, or a nickel–cobalt alloy were prepared with $[St]_{117}[HEMA]_{21}$ diblock copolymer (Scheme 1); the details are described in a previous report.[15]

Analysis

The composition and structure of the PSt-*b*-PHEMA/metal hybrids were confirmed with infrared (IR) spectroscopy (Equinox 55, Bruker, Karlsruhe, Germany) with KBr pellets. Ultraviolet–visible (UV–vis) absorption spectra were obtained on a UV-2401 PC spectrophotometer (Sahimadzu Corp., Kyoto, Japan). Absorption from the medium was subtracted from each spectrum. Thermogravimetric analysis (TGA) was performed by TGA-50H (Sahimadzu) with alumina plates with about 9 mg of the sample under a nitrogen atmosphere at a heating rate of 10°C/min. Magnetic measurements for powder samples of several tens of milligrams were performed with a vibrating sample magnetometer (BHV-55, model VSM VT-800, Riken Densh Co., Ltd., Yokohama, Japan) at temperatures ranging from 78 to 423 K and at fields ranging from 0 to 5 kOe. All the data were corrected for the contribution of the sample holder.

RESULTS AND DISCUSSION

IR spectra of the PSt-*b*-phema/metal hybrids

Figures 1 and 2 present IR spectra of PSt-*b*-PHEMA/metal-ion complex hybrids and polymer/metal hybrids, respectively. The adsorption bands at 1604, 1493, and 1450 cm^{-1} and the double peak of 752 and 699 cm^{-1} are the characteristic band of PSt [Fig. 1(a)]. A band at 1726 cm^{-1} appears due to the C═O groups of PHEMA, and a strong band at 1156 cm^{-1} is due to the C—C—O groups of PHEMA. These results show that the copolymer was composed of PSt and PHEMA [Fig. 1(a)]. After PSt-*b*-PHEMA reacted with the metal, the intensity of the band at 1725 cm^{-1} decreased, and new bands appeared at 1630 [Fig. 1(b); PSt-*b*-PHEMA/nickel-ion complex, B-1], 1583 [Fig. 1(c); PSt-*b*-PHEMA/cobalt-ion complex, B-2], and 1583 cm^{-1} [Fig. 1(d); PSt-*b*-PHEMA/nickel–cobalt alloy ionic complex, B-3]. These results implied that a PSt-*b*-PHEMA/nickel-ion complex, a PSt-*b*-PHEMA/cobalt-ion complex, and a PSt-*b*-PHEMA/nickel–cobalt-ion complex formed, respectively. After the PSt-*b*-PHEMA/metal complexes were reduced by KBH_4, there was no visible change in the adsorption band position, but the intensity of these adsorption bands had greatly decreased; this suggested a large reduction in the PSt-*b*-PHEMA/metal-ion complex. These results agree with our previous XRD and ESCA results.[15] Nickel and cobalt metal existed after the PSt-*b*-PHEMA/metal-ion complexes were reduced by KBH_4 according to the XRD results. ESCA analysis showed that nanometer metal particles [Ni (0) or Co (0)] on the surface formed and oxidized easily in air to form NiO or CoO. Furthermore, UV–vis spectra of the PSt-*b*-PHEMA/metal complexes and PSt-*b*-PHEMA/metal hybrids were measured.

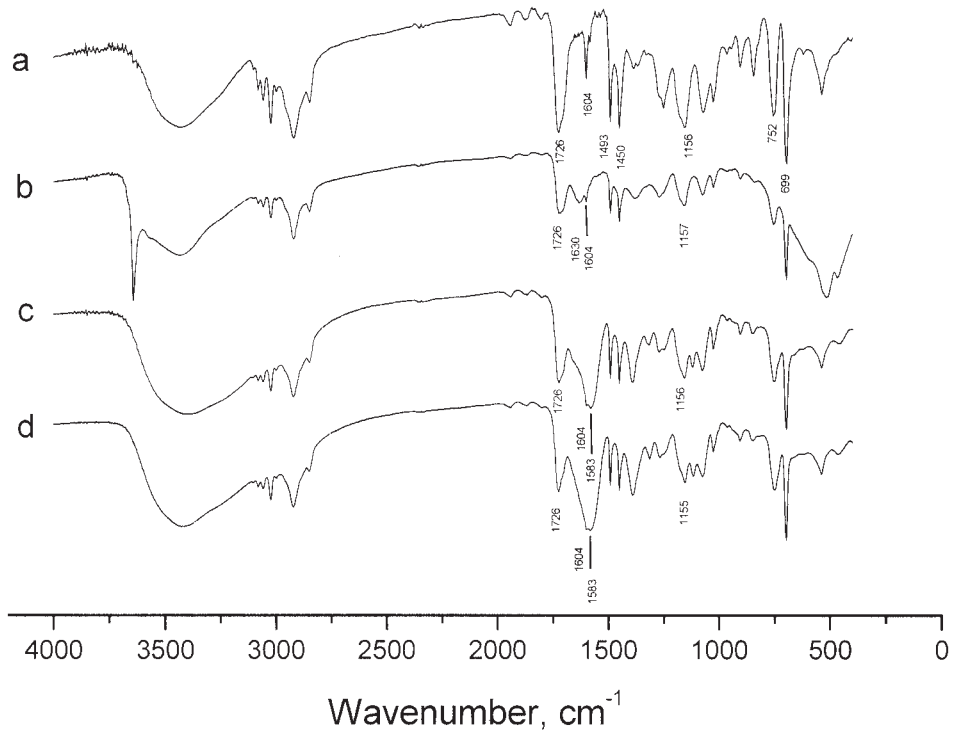

Figure 1 IR spectra of (a) PSt-*b*-PHEMA, (b) B-1, (c) B-2, and (d) B-3.

UV–vis data for the PSt-*b*-phema/metal hybrids

Table I shows the UV–vis absorption wavelength (λ_m) of the PSt-*b*-PHEMA/metal-ion complexes and PHEMA-*b*-PHEMA/metal hybrids. A comparison of these spectra shows that λ_m experienced a redshift after the reduction of the PSt-*b*-PHEMA/metal-ion complexes with KBH_4; among them, the PSt-*b*-PHEMA/nickel–cobalt alloy hybrids (B-33) had the longest redshift in comparison with the PSt-*b*-PHEMA/nickel hybrids (B-11) and PSt-*b*-PHEMA/cobalt hybrids (B-22), and PSt-*b*-PHEMA/nickel had the shortest redshift.

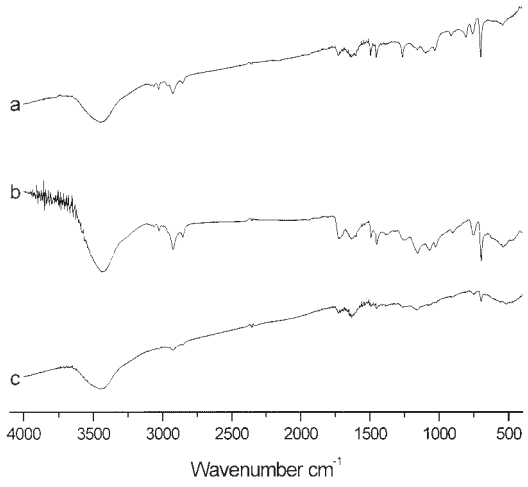

Figure 2 IR spectra of (a) B-11, (b) B-22, and (c) B-33.

Magnetic properties

Magnetic hysteresis loops of PSt-*b*-PHEMA/metal hybrids, as shown in Figures 3–5, were measured on powder samples at room temperature with a vibrating sample magnetometer. The saturation magnetization [M_s (emu/g of PSt-*b*-PHEMA/metal hybrids)], coercivity [H_c (Oe)], and remanent magnetization [M_r (emu/g of PSt-*b*-PHEMA/metal hybrids)] are given in Table I. The results showed that M_s and M_r of the PSt-*b*-PHEMA/cobalt hybrids were the biggest, and those of the PSt-*b*-PHEMA/nickel hybrids were the least.

TABLE I
Summary of the Properties of the Samples Produced in This Study

Sample	λ_m (nm)	$\Delta\lambda_m$ (nm)	M_s (emu/g)	M_r (emu/g)	H_c (Oe)
B-1	323.0				
B-11	326.5	3.5	0.73	0.36	348
B-2	315.0				
B-22	324.0	9.0	4.42	2.04	323
B-3	324.0				
B-33	343.0	19.0	3.41	1.84	292

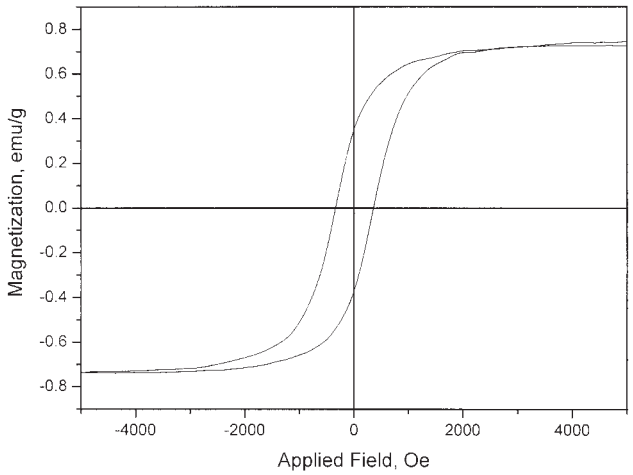

Figure 3 Magnetization versus the applied magnetic field (VSM curves) for PSt-*b*-PHEMA/nickel hybrids taken at room temperature [H_c = 348 Oe, M_r = 0.36 emu/g, M_s = 0.73 emu/g].

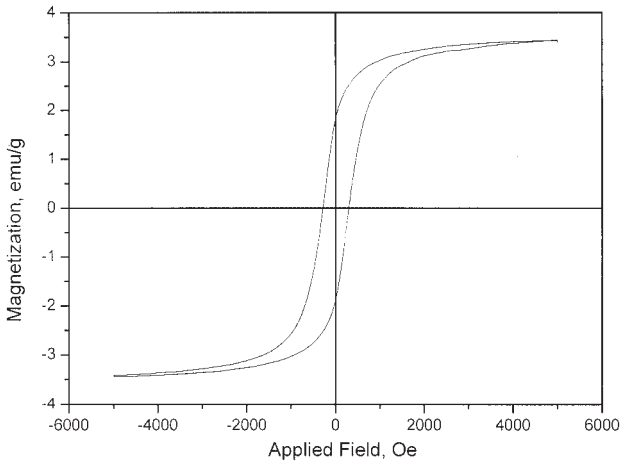

Figure 5 Magnetization versus the applied magnetic field (VSM curves) for PSt-*b*-PHEMA/nickel–cobalt alloy hybrids taken at room temperature [H_c = 292 Oe, M_r = 1.84 emu/g, M_s = 3.41 emu/g].

It is well known that bulk cobalt and nickel are ferromagnetic at room temperature. The results of our experiments showed that the PSt-*b*-PHEMA/metal hybrids had ferromagnetic properties. According to TEM results,[15] the obtained PSt-*b*-PHEMA ($[St]_{117}[HEMA]_{21}$) formed micellar aggregates with the insoluble block PSt as the core (20-nm diameter) and the soluble block PHEMA as the corona (10-nm thickness) in the mixed solvents DMF and water. When metal ions were added to this polymer solution, the metal complexed with the —OH group of PHEMA and prevented the PHEMA segment from aggregating around the core. After the block copolymer/metal-ion complexes (B-1, B-2, and B-3) were reduced by $NaBH_4$, the corresponding block polymer supported metal composites, PSt-*b*-PHEMA/nickel (B-11), PSt-*b*-PHEMA/cobalt (B-22), and PSt-*b*-PHEMA/nickel-Co (B-33) were obtained. XRD and ESCA analysis[15] showed the existence of nickel in B-11, cobalt in B-22, and a cobalt–nickel alloy in B-33. Magnetic attractive forces combined with inherently large surface energies (>100 dyn/cm)[18] favor nanoparticle aggregation in magnetic dispersions.[19] Previous TEM[15] results demonstrated this situation and showed that the metal aggregated and its size was more than 20 nm. Hysteresis curves with different characteristics are necessary for various applications.[20] Permanent magnets require a large remanence and coercive force so that they retain their magnetization even when maltreated. Computer memory stores and similar devices require a well-defined switching field with a sharp change between the positive and negative magnetizations, so they should have a very square hysteresis curve. Transformer laminations need thin, high curves to avoid saturation, to minimize losses, and to ensure that there is maximum flux linkage between primary and secondary circuits. The hysteresis curves of the PSt-*b*-PHEMA/metal hybrids were thin and high, and so these materials might be used as transformer laminations.

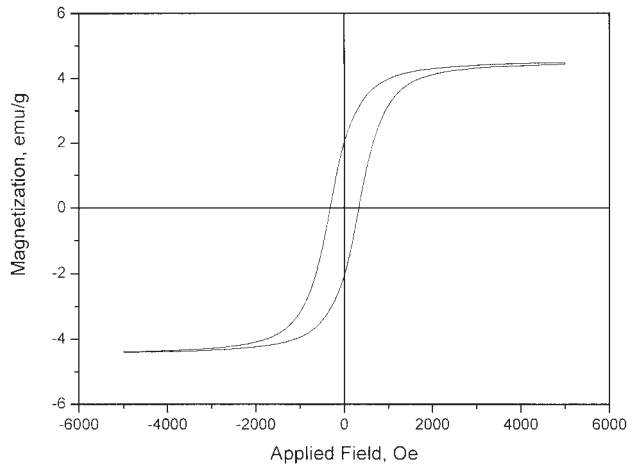

Figure 4 Magnetization versus the applied magnetic field (VSM curves) for PSt-*b*-PHEMA/cobalt hybrids taken at room temperature [H_c = 323 Oe, M_r = 2.04 emu/g, M_s = 4.42 emu/g].

Figure 6 present the magnetization curves of the PSt-*b*-PHEMA/metal hybrids. The magnetic intensity of the PSt-*b*-PHEMA/cobalt hybrids was the greatest in the whole range of applied fields (0–5000). These results mean that the PSt-*b*-PHEMA/cobalt hybrids were easier to magnetize than the PSt-*b*-PHEMA/nickel hybrids. In the case of the PSt-*b*-PHEMA/nickel–cobalt alloy hybrids, the magnetic intensity was lower than that of the PSt-*b*-PHEMA/cobalt hybrids; this was due to the lower cobalt content (5.96%) in comparison with the PSt-*b*-PHEMA/cobalt hybrids

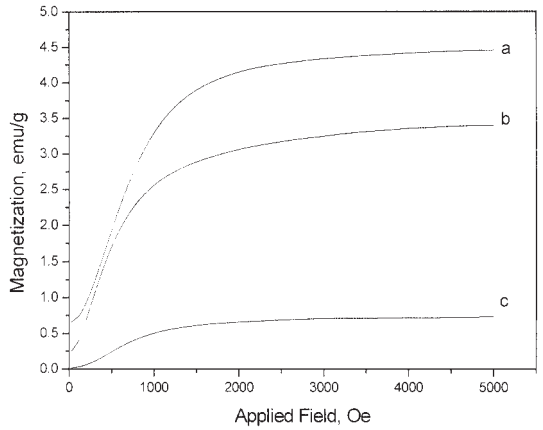

Figure 6 Magnetization curves of (a) B-22, (b) B-33, and (c) B-11.

(7.64%). Figure 7 shows the temperature dependence of the magnetic susceptibility [χ (emu/g of PSt-*b*-PHEMA/metal hybrids)] for B-11, B-22, and B-33. The χ values of the PSt-*b*-PHEMA/cobalt hybrids [Fig. 7(a)] are the largest in the temperature range of 150–400 K in comparison with the PSt-*b*-PHEMA/nickel–cobalt alloy hybrids [Fig. 7(b)] and PSt-*b*-PHEMA/nickel hybrids [Fig. 7(c)]. Below 150 K, there are some undulations in curves a–c. However, when the temperature is above 400 K, the χ values of B-22 and B-33 increase with the temperature.

χ is defined in terms of the magnetization, M, produced by an applied magnetic field, H, as follows:

$$\chi = M/H \tag{1}$$

Generally,[20] below the Curie temperature (T_c), the magnetic material is subdivided into domains, each of which is spontaneously magnetized in agreement with eq. (2), but in which the direction of magnetization changes between one domain and the next:

$$M = M_0(1 - \alpha T^n) \tag{2}$$

where M_0 is the magnetization at 0 K, α is the constant if the magnetic materials are definite, and n is 3/2.

Thus, at a very low temperature ($\ll T_c$), the variations of χ are in agreement with eq. (2). Of course, all these theories are appropriate for inorganic magnetic materials. Magnetic PSt-*b*-PHEMA/metal hybrids are composed of a polymer and a metal (nickel, cobalt, or a nickel–cobalt alloy), so the variation in the regularity of χ with temperature may be different from that of pure inorganic magnetic materials. It is well known that the external factor of the polymer resulting in internal rotation is the environmental temperature. When a sample was first cooled at 78 K, 2500 Oe was applied, and the magnetization measurement was taken with increasing temperature. The process of magnetization of magnetic PSt-*b*-PHEMA/metal hybrids entails a change in the arrangement of the domains, so their magnetization becomes more nearly parallel, the rotation of the molecules begins freer, and the polymer chains become more flexible. However, below 150 K, this process is not finished completely, and so there are some undulations in the curve [Fig. 7(a–c)]. From 150 to 400 K, the variations of χ are in agreement with eq. (2). When the temperature is above 400 K, χ increases with the temperature; this means that some block copolymer begins to decompose because of the lower glass temperature of PHEMA (ca. 63°C; the data are not shown). Thus, the metals, especially cobalt, like to aggregate. To investigate these speculations, TGA of B-11, B-22, and B-33 was performed. When the samples were heated at 400 K, percentage of thermal weight loss (Δm) was 97.5 (B-11), 93.3 (B-22), and 95.6% (B-33). These results implied that the metal aggregated at this temperature because of the beginning decomposition of the block copolymer. The reason that the weight loss of the PSt-*b*-PHEMA/cobalt hybrids (B-22) was bigger than that of the PSt-*b*-PHEMA/nickel hybrids (B-11) at the same temperature is not clear.

CONCLUSIONS

A redshift happened after the PSt-*b*-PHEMA/metal-ion complexes were reduced by KBH_4. The PSt-*b*-PHEMA/nickel–cobalt alloy hybrids had the biggest redshift ($\Delta\lambda_m$ = 19.9 nm) in comparison with the PSt-*b*-PHEMA/nickel hybrids ($\Delta\lambda_m$ = 3.5 nm) and PSt-*b*-PHEMA/cobalt hybrids ($\Delta\lambda_m$ = 9.0 nm). The PSt-*b*-PHEMA/metal hybrids had the hysteresis phenomenon at room temperature, which showed that the PSt-*b*-PHEMA/nickel, PSt-*b*-PHEMA/cobalt, and PSt-*b*-PHEMA/nickel–cobalt were ferromagnetic materials.

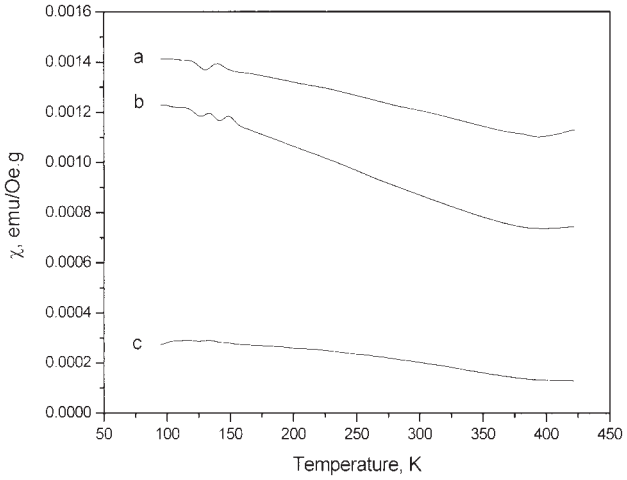

Figure 7 χ with an applied field of 2500 Oe for (a) B-22, (b) B-33, and (c) B-11.

H_c of the PSt-*b*-PHEMA/nickel hybrids was 348 Oe, M_s was 0.73 emu/g, and M_r was 0.36 emu/g. H_c of the PSt-*b*-PHEMA/cobalt hybrids was 323 Oe, M_s was 4.42 emu/g, and M_r was 2.04 emu/g; H_c of the PSt-*b*-PHEMA/nickel–cobalt alloy hybrids was 292 Oe, M_s was 3.41 emu/g, and M_r was 1.84 emu/g. The PSt-*b*-PHEMA/cobalt hybrids were easier to magnetize than the PSt-*b*-PHEMA/nickel hybrids. χ of the PSt-*b*-PHEMA/metal hybrids decreased with increasing temperature in the range of 150–400 K and increased with the temperature above 400 K.

References

1. Qian, X. F.; Yin, J.; Yang, Y. F.; Lu, H.; Zhu, Z. K.; Lu, J. J Appl Polym Sci 2001, 82, 2744.
2. Saito, R.; Okamura, S.; Ishizu, K. Polymer 1996, 37, 5255.
3. Vijaya Kumar, R.; Koltypin, Y.; Palchik, O.; Gedanken, A. J Appl Polym Sci 2002, 86, 160.
4. Yue, J.; Cohen, R. E. Supramol Sci 1994, 1, 117.
5. Moffitt, M.; Eisenberg, A. Chem Mater 1995, 7, 1178.
6. Moffitt, M.; Mcmahon, L.; Pessel, V.; Eisenberg, A. Chem Mater 1995, 7, 1185
7. Antonietti, M.; Wenz, E.; Bronstein, L.; Seregina, M. Adv Mater 1995, 7, 1000.
8. Chan, Y. N. C.; Schrock, R. R.; Cohen, R. E. Chem Mater 1992, 4, 24.
9. Cummins, C. C.; Schrock, R. R.; Cohen, R. E. Chem Mater 1992, 4, 27.
10. Chan, Y. N. C.; Schrock, R. R.; Cohen, R. E. J Am Chem Soc 1992, 114, 7295.
11. Chan, Y. N. C.; Craig, G. S. W.; Schrock, R. R.; Cohen, R. E. Chem Mater 1992, 4, 885.
12. Sohen, B. H.; Cohen, R. E. J Appl Polym Sci 1997, 65, 723.
13. Abes, J. I.; Cohen, R. E.; Ross, C. A. Chem Mater 2003, 15, 1125.
14. Abes, J. I.; Cohen, R. E.; Ross, C. A. Mater Sci Eng C 2003, 23, 641.
15. Wang, Y.; Wu, J.; Yuan, J.; Sun, G.; Pan, C. J Appl Polym Sci 2002, 83, 2883.
16. Wang, J. S.; Matyjaszewsk, K. J Am Chem Soc 1995, 117, 5614.
17. Wang, J. S.; Matyjaszewsk, K. Macromolecules 1995, 28, 7901.
18. Kim, D. K.; Zhang, Y.; Voit, W.; Rao, K. V.; Muhammed, J. Magn Magn Mater 2001, 225, 30.
19. Harris, L. A.; Goff, J. D.; Carmichael, A. Y.; Riffle, J. S.; Harburn, J. J.; St. Pieerre, T. G.; Saunders, M. Chem Mater 2003, 15, 1367.
20. Rosenberg, H. M. The Solid State, 2nd ed.; Oxford University Press: New York, 1978; Chapter 12.